Identification of an appropriate cell line for the renal cell carcinoma model

In Youb Chang
Chosun University College of Medicine
Takbum Ohn
Chosun University College of Medicine
Daeun Moon
Jeju National University
Young Hee Maeng
Jeju National University School of Medicine
Bo Gun Jang
Jeju National University School of Medicine
Sang-Pil Yoon (spyoon@jejunu.ac.kr)
Jeju National University School of Medicine` https://orcid.org/0000-0003-1350-3582

Primary research

Keywords: Ferroptosis, Renal cell carcinoma, SNU-333, Resistance, Orthotopic model

Posted Date: July 6th, 2020

DOI: https://doi.org/10.21203/rs.3.rs-39971/v1

Abstract

Background Although renal cell carcinoma (RCC) is known to be susceptible to ferroptosis, we found primary RCC cells showed resistance to ferroptosis and aimed to investigate a feasible candidate for an appropriate cell line for the RCC model. Methods Glutathione peroxidase 4 (GPX4) immunostaining was adopted in the RCC tissue microarrays. Normal human proximal tubule cells (HK-2) and RCC cell lines were used for the MTT assay, Western blotting, sphere-forming assay, and orthotopic injection of athymic Balb/c-nude mice. Results GPX4 immunostaining showed low intensity compared to the normal kidney, which coincided with the ferroptosis-susceptibility of RCC. Primary RCC cell lines (Caki-2, SNU-333, SNU-349, and SNU-1272) showed resistance to 5-fluorouracil and a GPX4 inhibitor compared to the HK-2 cells and to metastatic RCC cells (Caki-1). The Caki-2 cells showed increased GPX4 and xCT, and the SNU-333 cells showed increased ferritin heavy chain (FTH1) compared to the other RCC cells. The Caki-2 cells showed increased aSMA, fibronectin, vimentin, and SNAIL, and the SNU-333 cells showed increased aSMA, E-cadherin, and EpCAM. The Caki-2 cells showed increased Sox-2 and CD105, and the SNU-333 cells showed increased c-Myc and Lgr5. The Caki-1 and SNU-333 cells formed spheres in vitro and orthotopic RCC masses in vivo. The injected SNU-333 tumor only showed high intensities of CD10 and PAX8, consistent with the diagnostic criteria for RCC. Conclusions The primary RCC cell lines used in this study were more resistant to ferroptosis and 5-fluorouracil, and the SNU-333 cells showed tumor-initiating capacities in vitro and in vivo. These results suggest that SNU-333 might be suitable as a orthotopic RCC model for future research.

Background

Renal cell carcinoma (RCC), originates from the proximal tubule [1], shows an increasing incidence of ~ 21.7 per 100,000 people over the last decade in the Republic of Korea [2]. RCC is not sensitive to conventional chemotherapy and is at least partly resistant to apoptosis [3], but known among the cancer cell lines to be susceptible to lipid repair enzyme GPX4-regulated ferroptosis [4]. Ferroptosis is a specific form of programmed cell death, which is initiated by an increase in the labile iron pool and lipid reactive oxygen species (ROS) production [5–7]. The chelation of iron by deferoxamine rescues the experimental induction of ferroptosis [8], but inhibition of the cysteine uptake (system Xc^- (xCT)) by erastin or sulfasalazine or the inactivation of GPX4 by (1S,3R)-2-(2-chloroacetyl)-2,3,4,9-tetrahydro-1-[4-(methoxycarbonyl)phenyl]-1H-pyrido[3,4-b]indole-3-carboxylic acid, methyl ester (RSL3) induces ferroptosis [5, 7]. In this context, changes in iron profiles, such as serum iron, ferritin, and transferrin receptor (TfRC), have been suggested as successful markers for chemotherapy for metastatic RCC [9], and a variety of iron metabolism genes were significantly associated with the survival of RCC patients [10].

The resistance of RCC might be associated with the characteristics of cancer stem cells (CSCs). CSCs, which present characteristics reminiscent of normal stem cells (i.e., Oct4, Sox2, c-Myc, and Lgr5), show common features that include maintenance of the stem cell pool (self-renewal), tumorigenesis, and metastasis *in vivo*, and treatment resistance and recurrence [11, 12]. According to the CSC hypothesis,

conventional chemotherapies usually cannot eliminate the CSC pool [13], which may cause tumor recurrence. Several RCC markers were found to be specifically expressed in CSCs, such as CD105, ALDH1, and Oct4, although CSC markers are not unique across tumor types [12, 14]. In addition, tumor cells in the non-CSC subpopulation can spontaneously undergo epithelial-mesenchymal transition (EMT) and acquire a CSC-like phenotype and surface marker expression [15–17]. High expression of CD44 in RCC also correlated with recurrence and poor prognosis for 5-year overall survival [18].

In our previous report [19], yeast extract treatment decreased TfRC and increased ferritin in metastatic RCC cells, but decreased GPX4 in primary RCC cells. Altered iron metabolism may differentially contribute to growth inhibition or ferroptosis induction in various RCC cell lines since iron itself contributes to mutagenicity and malignant transformation, and the transformed malignant cells require high amounts of iron for proliferation [6, 20]. Herein, we aimed to investigate a feasible candidate for an appropriate cell line for RCC model since most RCCs remain resistant cancers against various cell death-related therapeutic strategies.

Materials And Methods

Reagents and antibodies

3-[4,5-Dimethylthiazol-2-yl]-2,5-diphenyl tetrazolium bromide (MTT) was purchased from Amresco, Inc. (VWR International LLC, Seongnam, Republic of Korea). Deferoxamine mesylate, 5-fluorouracil (5-FU), poly-2-hydroxyethyl methacylate, and sulfasalazine were purchased from Sigma-Aldrich (Merck KGaA, Darmstadt, Germany), and RSL3 was purchased from APExBIO Technology (Houston, TX, USA). Epidermal growth factor (EGF) and basic fibroblast growth factor (bFGF) were purchased from Gibco (ThermoFisher Scientific, Seoul, South Korea), and B27 supplement was purchased from Invitrogen (Thermo Fisher Scientific). The ALDH activity assay kit (colorimetric) was purchased from Abcam (Cambridge, MA, USA).

The antibodies specific for β-actin (C-4) (diluted 1:2,000), c-Myc (9E10) (diluted 1:1,000), E-cadherin (H-108) (diluted 1:1,000), EpCAM (c-10) (diluted 1:1,000), ferritin heavy chain (B-12) (FTH1; diluted 1:2,000), Oct3/4 (C-10) (diluted 1:1,000), SNAIL (G-7) (diluted 1:1,000), Sox2 (E-4) (diluted 1:1,000), transferrin receptor (H68.4) (CD 71, TfRC; diluted 1:2,000), and vimentin (V9) (diluted 1:1,000) were purchased from Santa Cruz Biotechnology (Santa Cruz, CA, USA); CD24 [M1/69] (diluted 1:1,000), CD44 (diluted 1:1,000), CD105 (diluted 1:1,000), EGFR [EP38Y] (diluted 1:1,000), glutathione peroxidase 4 (GPX4 [EPNCIR144]; diluted 1:1,000), Lgr5 [EPR3065Y] (diluted 1:500), and SLC40A1 (ferroportin, FPN; diluted 1:1000) were purchased from Abcam; and α-smooth muscle actin (diluted 1:2,000; Sigma-Aldrich), CD10 antibody (SP67) (ready for use; Ventana; Tucson, AZ, USA), CD44-variant 9 (CD44v9/1459) (diluted 1:1,000; Novus Biologicals, CO, USA), fibronectin (diluted 1:2,000; Cedarlane, Canada), PAX8 (MRQ-50) (ready for use; Roche Diagnostics, Seoul, South Korea), and SLC7A11 (cysteine/glutamate transporter (xCT); diluted 1:2,000; Alomone Labs, Jerusalem, Israel) were purchased as indicated.

Cell culture

Human kidney proximal tubule cells (HK-2) and RCC cells (Caki-1, Caki-2, SNU-333, SNU-349, and SNU-1272) were purchased from the Korean Cell Line Bank (Seoul, Republic of Korea), and cultured according to the supplier's protocol. The HK-2, SNU-333, SNU-349, and SNU-1272 cells were cultured in RPMI-1640 medium, and Caki-1 and Caki-2 cells were cultured in DMEM/high glucose. All media were from Welgene (Gyeongsan, Republic of Korea) and contained 10% fetal bovine serum (FBS) and 1% penicillin-streptomycin. The cells were grown in monolayers at 37 ℃ in a 5% CO_2 incubator otherwise described.

MTT assay

The effect of drugs on cell viability was evaluated by MTT reduction to its formazan product. The cells were seeded in triplicate wells of 96-well plates (2 x 10^3 cells/well), and treated with 5-fluorouracil, RSL3, sulfasalazine, and deferoxamine at various concentrations. The cells were incubated for three days and then 10 µl of the MTT reagent (5 mg/ml in PBS) was added to each well, dissolved in DMSO for 15 min, and the MTT reduction was measured 3 h later spectrophotometrically at 595 using the absorbance at 620 nm as background by a VERSAmax microplate reader (Molecular Devices Korea LLC). The absorbance values obtained from the wells of the untreated cells represented 100 % cell viability and were used for comparison to the treated cells.

Sphere-forming assay

The sphere-forming assays were conducted as previously reported [21,22] with a slight modification. In brief, single-cell suspensions were plated in 96-well plates covered with poly-2-hydroxyethyl methacylate to prevent cell attachment, at a density of 5 x 10^2 cells in serum-free DMEM/F12 medium supplemented with 1% B27 supplement, 20 ng/ml EGF, and 20 ng/ml bFGF. After 15 days in culture, the number and the size of the spheres per well were acquired.

ALDH1 activity assay

The aldefluor assay was performed according to the manufacturer's instructions (Abcam) [23]. Briefly, we labeled one TEST and one CONTROL tube for each sample. We lysed the cells and add activated ALDEFLUOR reagent to the lysed cell suspensions and 5 µl of DEAB to the CONTROL tube and then transferred to the TEST tube, mixed and immediately transferred 0.5 ml of the mixture to the CONTROL tube. The test samples were incubated at 37 °C, centrifuged, and resuspended in assay buffer. Finally, ALDH activity was measured spectrophotometrically at 450 nm using a VERSAmax microplate reader (Molecular Devices Korea, LLC). The absorbance values obtained from the HK-2 cells represent 100% activity and were used for comparison to the RCC cells.

Western blotting

To obtain the intracellular proteins, cultured cells were harvested in M-PER mammalian protein extraction reagent (Thermo Fisher Scientific) including 1% protease inhibitor cocktail set III (EMD Millipore), 0.5% phosphatase inhibitor cocktail 2, and 0.5% phosphatase inhibitor cocktail 3 (both from Sigma-Aldrich).

The protein concentrations were assessed using BCA protein assay (ThermoFisher Scientific) according to the manufacturer's instructions.

Electrophoresis of the protein in cell lysates was performed with the TGX Stain-Free FastCast™ Acrylamide Starter Kit (Bio-Rad Laboratories, Inc., Seoul, South Korea) using a Tris/glycine buffer system (Bio-Rad Laboratories) and transferred onto PVDF membranes as previously described [19]. The membranes were blocked with 5% skim milk for 1 h and then incubated with primary antibodies overnight at 4 °C. After washing, peroxidase anti-mouse or anti-rabbit IgG antibodies (Vector Laboratories, Inc., Seoul, South Korea) were applied for 1 h at room temperature. Next, Western Lightning Chemiluminescence Reagent (PerkinElmer, Inc., Daejeon, South Korea) was used to detect the proteins. Anti-GAPDH antibody was used as a loading control on the stripped membranes. The bands were quantified using AzureSpot analysis software (version 14.2; Azure™ c300; Azure Biosystems, Inc. Dublin, CA, USA).

Orthotopic RCC model establishment

All animal experiments were conducted in accordance with and approved by the Jeju National University Institutional Animal Care and Use Committee (2019-0015).

Athymic Balb/c nude mice (7-week-old males) were purchased from OrientBio (Seongnam, Republic of Korea). To induce an orthotopic RCC model, the mice were divided into five groups (n = 5 mice/group) according to the different RCC cell lines (Caki-1, Caki-2, SNU-333, SNU-349, and SNU-1272), and anesthetized using an intraperitoneal injection of sodium pentobarbital (Entobar^{TM}, Hanlim Pharm. Co. Ltd., Seoul, South Korea). Under aseptic conditions, a small longitudinal incision was made in the left lower back, and 2 x 10^5 cells in 20 µl of Matrigel (BD Biosciences, Becton Dickinson, Seoul, South Korea) were injected with a 27-gauge needle into the renal capsule. Thirty days following the injection, the mice were euthanized, the tumor masses explanted and fixed for 24 h in 4% paraformaldehyde, and the fixed tissues were dehydrated and embedded in paraffin wax. Sections (4 µm-thick) were cut with a microtome and prepared for hematoxylin/eosin (H/E) staining and immunohistochemistry.

Immunohistochemistry

Commercially available patient kidney tissue arrays (CL2) from SuperBioChips Laboratories (Seoul, Republic of Korea) were used for immunohistochemistry (IHC). GPX4 IHC was performed according to the supplier’s protocol. Each array contains 50 tumor sections and nine matched control sections. As a primary antibody, we used a polyclonal rabbit anti-human GPX4 antibody (1:2000, Abcam). GPX4 was visualized by staining with a biotinylated anti-rabbit secondary antibody (1:200, Vector Laboratories), developed with diaminobenzidine, and counterstained with hematoxylin. Blind-scoring for the GPX4 immunostaining was performed by two independent observers who first assessed the overall staining intensity on a single array. Next, we used a 4-step scoring scale to score the individual sections: 0 for absent or very low, 1 for mild staining, 2 for moderate staining, and 3 for strong staining.

For the primary antibodies, CD 10 and paired box G8 (PAX8), used for diagnosing RCC [24], we used the Benchmark XT staining system (Roche Diagnostics) on the orthotopic RCC masses, developed with DAB and counterstained with hematoxylin.

Statistical analysis

All data were compiled from a minimum of three replicate experiments. The data are expressed as mean values ± SD. Statistically significant differences ($p < 0.05$) were obtained using the Student *t*-test or one-way analysis of variance (ANOVA) with a Bonferroni post-hoc test (MS excel 2010).

Results

RCCs are known to be susceptible to ferroptosis, but primary RCCs show resistance to ferroptosis

To confirm the susceptibility of RCC to ferroptosis, GPX4 immunostaining of human RCC tissues was done. The GPX4 immunostaining scores of the human RCC tissues were 2.89 ± 0.11 for normal, 1.98 ± 0.15 for Stage I, 2.14 ± 0.15 for Stage II, 2.14 ± 0.14 for Stage III, and 1.75 ± 0.25 for Stage IV. The staining intensity was significantly lower in RCC tissue compared to normal human kidney ($p < 0.001$), in which metastatic stage IV was the lowest, without significance (Fig. 1A).

To confirm the known characteristics of RCC, the effects of an anti-cancer drug (5-FU), inducers of ferroptosis (RSL3 and sulfasalazine), and an inhibitor of ferroptosis (deferoxamine) on cell viability were assessed using the MTT assay (Fig. 1B).

The anticipated IC_{50} values of the HK-2, Caki-1, Caki-2, SNU-333, SNU-349, and SNU-1272 cells with 5-FU were 4.7–37.2, 45.6–166.7, 165.3, 207.3, 281.0, and 125.2 μM, respectively. All RCC cell lines showed considerably higher IC_{50} values with 5-FU compared to the HK-2 cells, and the primary RCC cell lines also showed significance when compared to the Caki-1metastatic RCC cells.

The anticipated IC_{50} values of the HK-2, Caki-1, Caki-2, SNU-333, SNU-349, and SNU-1272 cells with RSL3 were 0.05, 0.39, 0.45, 4.16, 0.46, 0.44 μM, respectively. All RCC cell lines showed considerably higher IC_{50} values with RSL3 compared to the HK-2 cells, and the primary RCC cell lines also showed significance when compared to the metastatic RCC Caki-1 cells.

The anticipated IC_{50} values of the HK-2, Caki-1, Caki-2, SNU-333, SNU-349, and SNU-1272 cells with sulfasalazine were 2.7, 0.4–1.5, 2.45, 2.70, 2.89, 2.60 mM, respectively. All primary RCC cell lines showed similar IC_{50} values with sulfasalazine and the metastatic RCC Caki-1 cells only showed significantly lower IC_{50} values compared to the HK-2 cells. All primary RCC cell lines showed significantly higher IC_{50} values compared to the Caki-1 cells.

The anticipated IC_{50} values of the HK-2, Caki-1, Caki-2, SNU-333, SNU-349, and SNU-1272 cells with deferoxamine were 55.3, 35.2, 53.8, 289.8, 370.9, 48.7 μM, respectively. The metastatic RCC Caki-1 cells showed significantly lower IC_{50} values as compared to the HK-2 cells, but the primary RCC cell lines showed considerably higher IC_{50} values than the HK-2 and Caki-1cells.

Ferroptosis-resistant Caki-2 and SNU-333 cells show increased levels of CSC or tumor markers

As the primary RCC cells showed resistance to ferroptosis and an anti-cancer drug compared to the HK-2 and metastatic RCC cells, ferroptosis-related markers were first assessed in the RCC cell lines (Fig. 2A). Compared to the HK-2 cells, the Caki-2 cells only showed significantly increased levels of GPX4 and xCT ($p < 0.05/.0124, 0.0465$), whereas Caki-1, SNU-349, and SNU-1272 showed considerably decreased levels. The transferrin receptor (TfRC), ferritin heavy chain (FTH1), and ferroportin (FPN) levels were analyzed. The Caki-2 cells showed significantly increased levels of TfRC ($p < 0.05/0.0179$) and FTH1 ($p < 0.05/0.0108$), whereas the Caki-1 ($p < 0.001$), SNU-349 ($p < 0.01/.00144$), and SNU-1272 ($p < 0.001$) cells showed considerably decreased levels of TfRC. The SNU-349 ($p < 0.05/.0416$) and SNU-1272 ($p < 0.05/ 0.0151$) cells showed significantly decreased levels of FPN. Interestingly, the SNU-333 cells showed significantly increased levels of FTH1 ($p < 0.01/ 0.0060$). The levels of the other markers were comparable to those in the HK-2 cells.

Next, cancer stem markers and tumor markers were assessed in the RCC cell lines (Fig. 2B). Compared to the HK-2 cells, the Caki-2 cells only showed significantly increased levels of Sox2 ($p < 0.001$), c-Myc ($p < 0.05/.0288$), and CD105 ($p < 0.01/ 0.0011$), and the Caki-1 cells only showed considerably increased levels of Sox2 ($p < 0.05/ 0.0165$). The SNU-333 cells showed significantly increased levels of Sox2 ($p < 0.05/0.0123$), c-Myc ($p < 0.001$), and Lgr5 ($p < 0.05/ 0.0318$). The SNU-349 cells showed considerably increased levels of c-Myc ($p < 0.01/ 0.0013$).

Surface markers were also assessed in the RCC cell lines (Fig. 2C). Compared to the HK-2 cells, the Caki-2 cells showed significantly increased levels of CD24 ($p < 0.05/ 0.0123$) and CD44 ($p < 0.01/ 0.0036$). The others were not changed considerably or decreased.

Tumorigenic capacity was significant in Caki-1 and SNU-333 cells in vitro

To check the relationship between resistance and tumorigenic capacity, the RCC cell lines were cultured in serum-free media supplemented with growth factors (Fig. 3A). Following two weeks of *in vitro* culture, only the Caki-1 and SNU-333 cells successfully formed spheres. The respective number of renospheres in the Caki-1, Caki-2, SNU-333, SNU-349, and SNU-1272 was 26.3 ± 1.6, 28.3 ± 2.2, 11.9 ± 1.2, 8.8 ± 0.7, 15.0 ± 1.1, respectively, which was significantly lower in the SNU-333, SNU-349, and SNU-1272 cells than the Caki-1 cells ($p < 0.001$). The mean size of the renospheres in each RCC cell line (listed above) was 134.5 ± 6.7, 96.2 ± 4.3, 158.2 ± 5.0, 83.0 ± 2.8, 81.0 ± 2.0 μm, respectively, in which the SNU-333 cells only showed significantly larger diameters when compared to the Caki-1 cells ($p < 0.01/.0052$). In addition, the SNU-333 cells showed the highest percentage of large spheres (92.1% of spheres larger than 100 μm) compared to the Caki-1 cells (74.2%).

EGFR expression was assessed (Fig. 3B) since EGF was supplemented for sphere formation. Compared to the HK-2 cells, the Caki-2 ($p < 0.001$) and SNU-333 ($p < 0.01/0.0011$) cells showed significantly higher EGFR expression among the RCC cell lines.

ALDH activity was assessed using the HK-2 cells as a control. The RCCs did not show any significant increase but were considerably decreased, except for the Caki-2 cells. The Caki-2 ($p < 0.001$) and SNU-333 ($p < 0.01$; 0.0017) cells were significantly increased compared to the Caki-1 cells.

As sphere forming assay inhibits adhesion of cells to the base of culture dish as a monolayer, EMT markers were assessed (Fig. 3C). All RCC cell lines showed significantly higher levels of αSMA ($p < 0.001$) compared to the HK-2 cells. The Caki-2 cells showed significantly increased levels of fibronectin ($p < 0.01/.0065$), vimentin ($p < 0.05/.0109$), and SNAIL ($p < 0.05/.0115$), but decreased levels of E-cadherin ($p < 0.001$) compared to the HK-2 cells. The SNU-333 cells showed significantly increased levels of E-cadherin ($p < 0.001$) and EpCAM ($p < 0.01/.0047$) compared to the HK-2 cells.

Tumorigenic capacity was further confirmed in Caki-1 and SNU-333 cells in vivo

To establish an orthotopic RCC model similar to human RCC, RCC cells were orthotopically injected into Balb/c nude mice (Fig. 4A). Among the RCC cell lines, the Caki-1 and SNU-333 cells successfully formed tumor masses.

We evaluated the morphological features by H/E staining, and the expression of markers with diagnostic relevance, such as CD10 and PAX8 (Fig. 4B). The Caki-1-bearing tumors consisted of spindle tumor cells with marked nuclear pleomorphism and desmoplasia and showed focal CD10 and PAX8 immunopositivity. The SNU-333-bearing tumors consisted of epithelioid tumor cells with clear or granular cytoplasm and showed strong CD10 and PAX8 immunopositivity. Based on the H/E and CD10 and PAX8 immunostaining results, the SNU-333 cell line showed the typical staining patterns of human RCC, whereas it was unclear if the Caki-1 cells originated from RCC. In addition, the GPX4 immunostaining was considerably weaker in both orthotopic tumor masses compared to the normal murine kidney.

Discussion

We found that among primary RCC cell lines, the SNU-333 cell line showed resistance to ferroptosis and was suitable for an orthotopic RCC model with tumorigenic capacities.

First, we confirmed that metastatic RCC was resistant to 5-FU, but susceptible to ferroptosis based on immunohistochemistry and MTT assay, as previously reported [3–5, 7, 8]. Interestingly, primary RCCs, especially the Caki-2 and SNU-333 cells, showed resistance to ferroptosis and 5-FU compared to metastatic RCC and/or the normal proximal tubule cells. The resistance to ferroptosis was related to GPX4, rather than xCT, and with deferoxamine (Fig. 1).

The Caki-2 cells showed significantly increased levels of GPX4 and xCT compared to the other cell lines, which may be the basic mechanism for the resistance to ferroptosis. However, the SNU-333 cells did not

show considerable changes with GPX4 or xCT (Fig. 2A). The GPX4-mediated resistance to ferroptosis in the Caki-2 cells might be reinforced by recent studies [25, 26] reporting that a GPX4-dependent cancer cell state underlies the clear cell morphology and confers sensitivity to ferroptosis. The clear cell morphology of RCCs is caused by highly active lipid and glycogen synthesis and deposition and marked by clear cytoplasm in histological analyses, which is hypersensitive to GPX4 knockdown [25]. The clear cell histotype shows vulnerability to ferroptosis via GPX4 dependency [26]. In addition, the Caki-2 cells showed significantly increased levels of TfRC and FTH1 and the SNU-333 cells showed increased levels of FTH1, which could be another mechanism for the resistance. Iron is usually dysregulated in cancers. Cancer cells often show higher levels of TfRC, down-regulation of FPN, and lower levels of ferritins, which lead to an increased intracellular labile iron pool [6, 20]. Although it is mostly utilized for tumor growth by cytosolic and mitochondrial iron enzymes, excessive amounts can promote increased oxidative stress via ROS accumulation and result in ferroptosis. The Caki-2 and SNU-333 cells showed paradoxically increased levels of ferritins (FTH1), which is comparable to a decreased intracellular labile iron pool and may lead to the resistance to ferroptosis.

Other resistance proteins, including CSC markers and tumor markers, were analyzed (Fig. 2B and 2C) because the primary RCCs also showed resistance to 5-FU compared to the metastatic RCC and/or HK-2 cells. Although the CSC markers are not unique across tumor types [12], normal stem cell markers (Oct4, Sox2, c-Myc, and Lgr5) and CSC markers (CD105) might share the characteristics of stem cells in RCCs [11, 12]. The Caki-2 cells showed increased levels of Sox2 and CD105, whereas the SNU-333 cells showed increased levels of c-Myc and Lgr5 compared to the other RCC cell lines. In addition, the Caki-2 cells only showed increased levels of CD24 and CD44. In the cell viability assay, the Caki-2 and SNU-333 cells showed stemness, which is associated with resistance and/or recurrence.

As non-CSCs can acquire a CSC-like phenotype during EMT [15, 16] and EMT-induced cells form spheres [17], a sphere-forming assay was conducted in the RCCs. As the Caki-1 cell line was reported to form more spheres compared to Caki-2 cells [22], the Caki-1 cells were considered a positive control. The SNU-333 cells only formed big renospheres, which were responsible for the significantly higher levels of EGFR (Fig. 3A and 3B). Mizumoto et al. [27] suggested that acquired resistance to sunitinib in RCC cells may be related to the activation of EGFR, and thus, increased EGFR in the SNU-333 cells might have a role in resistance, as well as sphere formation.

Compared to the Caki-1 cells, the Caki-2 and SNU-333 cells showed significantly increased ALDH1 activity (Fig. 3B), consistent with previous reports that CSCs could be identified with ALDH1 activity [12, 14]. Since the sphere-forming assay is anchorage-independent in culture [12], the EMT properties were examined (Fig. 3C). The RCCs showed significantly increased levels of αSMA, the Caki-2 cells showed increased fibronectin, vimentin, and SNAIL, and the SNU-333 cells showed increased E-cadherin and EpCAM. Taken together, the Caki-2 cells might show resistance via stemness and increased EMT-like properties. The SNU-333 cells also showed resistance via stemness but did not show EMT-like properties.

Finally, to evaluate the tumorigenic potential of RCCs *in vivo*, cancer cells are transplanted into immunocompromised mice. The Caki-1 and SNU-333 cells successfully formed orthotopic tumor masses, but the Caki-2 cells did not form tumors (Fig. 4A). The orthotopic masses were rarely immunostained with GPX4 while the normal tubules were stained, which was similar to the results of the human RCC tissue microarray. The histologic and immunohistochemical results revealed that the SNU-333 cells had characteristics consistent with the diagnostic criteria of human RCC (Fig. 4B). Metastatic RCC cells have been used to induce an orthotopic RCC model [24, 28, 29]. However, the established orthotopic RCC model might not be a proper model for ferroptosis-related research because metastatic RCC cells are known to be susceptible to ferroptosis. Using the proper cell line is crucial to furthering our understanding of RCC. Cancer is very complex and shows heterogeneity, and thus, choosing the right cell line for RCC research based on the molecular background has been suggested [30]. In addition to the well-known RCC cell lines (Caki-1 and Caki-2), we also used Korean RCC cell lines (SNU-333, SNU-349, and SNU-1272) primarily focused on the primary RCCs because we believe ferroptosis-resistant orthotopic RCC models are needed for further studies.

Conclusions

We clearly showed that the primary RCC cell lines were more resistant to ferroptosis than the metastatic RCC cells, in which the SNU-333 cell line showed resistance via iron metabolism and stemness, and further tumor-initiating capacities *in vitro* and *in vivo.* These results suggest that the SNU-333 cell line was the most suitable for a orthotopic RCC model for further research including the era of ferroptosis, drug resistance, and CSCs.

Abbreviations

5-FU, 5-fluorouracil

CSC, cancer stem cell

EMT, epithelial-mesenchymal transition

FTH1, ferritin heavy chain

GPX4, Glutathione peroxidase 4

MTT, 3-[4,5-Dimethylthiazol-2-yl]-2,5-diphenyl tetrazolium bromide

RCC, renal cell carcinoma

ROS, reactive oxygen species

RSL3, (1S,3R)-2-(2-chloroacetyl)-2,3,4,9-tetrahydro-1-[4-(methoxycarbonyl)phenyl]-1H-pyrido[3,4-b]indole-3-carboxylic acid, methyl ester

TfRC, transferrin receptor

xCT, cysteine/glutamate transporter system Xc^-

Declarations

Ethics approval and consent to participate

All animal experiments were conducted in accordance with and approved by the Jeju National University Institutional Animal Care and Use Committee (2019-0015).

Consent for publication

Not applicable

Availability of data and materials

The datasets used and/or analysed during the current study are available from the corresponding author on reasonable request.

Competing interests

The authors declare that they have no competing interests.

Funding

This study was supported by the Basic Science Research Program through the National Research Foundation of Korea (NRF) funded by the Ministry of Education (grant no. 2018R1D1A1A02050497).

Authors' contributions

OT, IYC and SPY conceived and designed the present study, and wrote the manuscript. OT, IYC, DM, YHM and BJ performed the experiments for data acquisition and analysis. OT, IYC and SPY interpreted the experimental results. All authors read and approved the final manuscript.

Acknowledgments

Not applicable.

References

1. Inamura K. Renal cell tumors: Understanding their molecular pathological epidemiology and the 2016 WHO classification. Int J Mol Sci. 2017;18(10):E2195. doi:10.3390/ijms18102195.
2. Koo KC, Chung BH. Epidemiology and treatment patterns of urologic cancers in Korea. Korean J Urol Oncol. 2015;13(2):51–7.

3. Toth C, Funke S, Nitsche V, Liverts A, Zlachevska V, Gasis M, et al. The role of apoptosis repressor with a CARD domain (ARC) in the therapeutic resistance of renal cell carcinoma (RCC): the crucial role of ARC in the inhibition of extrinsic and intrinsic apoptotic signalling. Cell Commun Signal. 2017;15(1):16. doi:10.1186/s12964-017-0170-5.
4. Yang WS, SriRamaratnam R, Welsch ME, Shimada K, Skouta R, Viswanathan VS, et al. Regulation of ferroptotic cancer cell death by GPX4. Cell. 2014;156(1–2):317–31. doi:10.1016/j.cell.2013.12.010.
5. Latunde–Dada GO. Ferroptosis. Role of lipid peroxidation, iron and ferritinophagy. Biochim Biophys Acta Gen Subj. 2017;1861(8):1893–900. doi:10.1016/j.bbagen.2017.05.019.
6. Pfeifhofer–Obermair C, Tymoszuk P, Petzer V, Weiss G, Nairz M. Iron in the tumor microenvironment–connecting the dots. Front Oncol. 2018;8:549. doi:10.3389/fonc.2018.00549.
7. Lai Y, Zeng T, Liang X, Wu W, Zhong F, Wu W. Cell death-related molecules and biomarkers for renal cell carcinoma targeted therapy. Cancer Cell Int. 2019;19:221. doi:10.1186/s12935-019-0939-2.
8. Dixon SJ, Lemberg KM, Lamprecht MR, Skouta R, Zaitsev EM, Gleason CE, et al. Ferroptosis: an iron-dependent form of nonapoptotic cell death. Cell. 2012;149(5):1060–72. doi:10.1016/j.cell.2012.03.042.
9. Golčić M, Petković M. Changes in metabolic profile, iron and ferritin levels during the treatment of metastatic renal cancer - A new potential biomarker? Med Hypotheses. 2016;94:148–50. doi:10.1016/j.mehy.2016.07.015.
10. Zhang S, Chang W, Wu H, Wang YH, Gong YW, Zhao YL, et al. Pan-cancer analysis of iron metabolic landscape across the Cancer Genome Atlas. J Cell Physiol. 2020;235(2):1013–24. doi:10.1002/jcp.29017.
11. Murphy AJ, Pierce J, de Caestecker C, Ayers GD, Zhao A, Krebs JR, et al. CITED1 confers stemness to Wilms tumor and enhances tumorigenic responses when enriched in the nucleus. Oncotarget. 2014;5(2):386–402. doi:10.18632/oncotarget.1566.
12. Corrò C, Moch H. Biomarker discovery for renal cancer stem cells. J Pathol Clin Res. 2018;4(1):3–18. doi:10.1002/cjp2.91.
13. Nguyen LV, Vanner R, Dirks P, Eaves CJ. Cancer stem cells: an evolving concept. Nat Rev Cancer. 2012;12(2):133–43. doi:10.1038/nrc3184.
14. Ueda K, Ogasawara S, Akiba J, Nakayama M, Todoroki K, Ueda K, et al. Aldehyde dehydrogenase 1 identifies cells with cancer stem cell-like properties in a human renal cell carcinoma cell line. PLoS One. 2013;8(10):e75463. doi:10.1371/journal.pone.0075463.
15. Kreso A, Dick JE. Evolution of the cancer stem cell model. Cell Stem Cell. 2014;14(3):275–91. doi:10.1016/j.stem.2014.02.006.
16. Shibue T, Weinberg RA. EMT, CSCs, and drug resistance: the mechanistic link and clinical implications. Nat Rev Clin Oncol. 2017;14(10):611–29. doi:10.1038/nrclinonc.2017.44.
17. Singla M, Kumar A, Bal A, Sarkar S, Bhattacharyya S. Epithelial to mesenchymal transition induces stem cell like phenotype in renal cell carcinoma cells. Cancer Cell Int. 2018;18:57. doi:10.1186/s12935-018-0555-6.

18. Li X, Ma X, Chen L, Gu L, Zhang Y, Zhang F, et al. Prognostic value of CD44 expression in renal cell carcinoma: a systematic review and meta-analysis. Sci Rep. 2015;5:13157. doi:10.1038/srep13157.
19. Moon D, Kim J, Yoon SP. Yeast extract inhibits the proliferation of renal cell carcinoma cells via regulation of iron metabolism. Mol Med Rep. 2019;20(4):3933–41. doi:10.3892/mmr.2019.10593.
20. Fanzani A, Poli M. Iron, oxidative damage and ferroptosis in rhabdomyosarcoma. Int J Mol Sci. 2017;18(8):E1718. doi:10.3390/ijms18081718.
21. Min SO, Lee SW, Bak SY, Kim KS. Ideal sphere-forming culture conditions to maintain pluripotency in a hepatocellular carcinoma cell lines. Cancer Cell Int. 2015;15:95. doi:10.1186/s12935-015-0240-y.
22. Micucci C, Matacchione G, Valli D, Orciari S, Catalano A. HIF2α is involved in the expansion of CXCR4-positive cancer stem-like cells in renal cell carcinoma. Br J Cancer. 2015;113(8):1178–85. doi:10.1038/bjc.2015.338.
23. Ouyang S, Zhou X, Chen Z, Wang M, Zheng X, Xie M. LncRNA BCAR4, targeting to miR-665/STAT3 signaling, maintains cancer stem cells stemness and promotes tumorigenicity in colorectal cancer. Cancer Cell Int. 2019;19:72. doi:10.1186/s12935-019-0784-3.
24. di Martino S, De Luca G, Grassi L, Federici G, Alfonsi R, Signore M, et al. Renal cancer: new models and approach for personalizing therapy. J Exp Clin Cancer Res. 2018;37(1):217. doi:10.1186/s13046-018-0874-4.
25. Miess H, Dankworth B, Gouw AM, Rosenfeldt M, Schmitz W, Jiang M, et al. The glutathione redox system is essential to prevent ferroptosis caused by impaired lipid metabolism in clear cell renal cell carcinoma. Oncogene. 2018;37(40):5435–50. doi:10.1038/s41388-018-0315-z.
26. Zou Y, Palte MJ, Deik AA, Li H, Eaton JK, Wang W, et al. A GPX4-dependent cancer cell state underlies the clear-cell morphology and confers sensitivity to ferroptosis. Nat Commun. 2019;10(1):1617. doi:10.1038/s41467-019-09277-9.
27. Mizumoto A, Yamamoto K, Nakayama Y, Takara K, Nakagawa T, Hirano T, et al. Induction of epithelial-mesenchymal transition via activation of epidermal growth factor receptor contributes to sunitinib resistance in human renal cell carcinoma cell lines. J Pharmacol Exp Ther. 2015;355(2):152–8. doi:10.1124/jpet.115.226639.
28. Gohji K, Nakajima M, Dinney C, Fan D, Pathak S, Killion J, et al. The importance of orthotopic implantation to the isolation and biological characterization of a metastatic human clear cell renal-carcinoma in nude-mice. Int J Oncol. 1993;2(1):23–32. doi:10.3892/ijo.2.1.23.
29. Berlato C, Khan MN, Schioppa T, Thompson R, Maniati E, Montfort A, et al. A CCR4 antagonist reverses the tumor-promoting microenvironment of renal cancer. J Clin Invest. 2017;127(3):801–13. doi:10.1172/JCI82976.
30. Brodaczewska KK, Szczylik C, Fiedorowicz M, Porta C, Czarnecka AM. Choosing the right cell line for renal cell cancer research. Mol Cancer. 2016;15(1):83. doi:10.1186/s12943-016-0565-8.

Figures

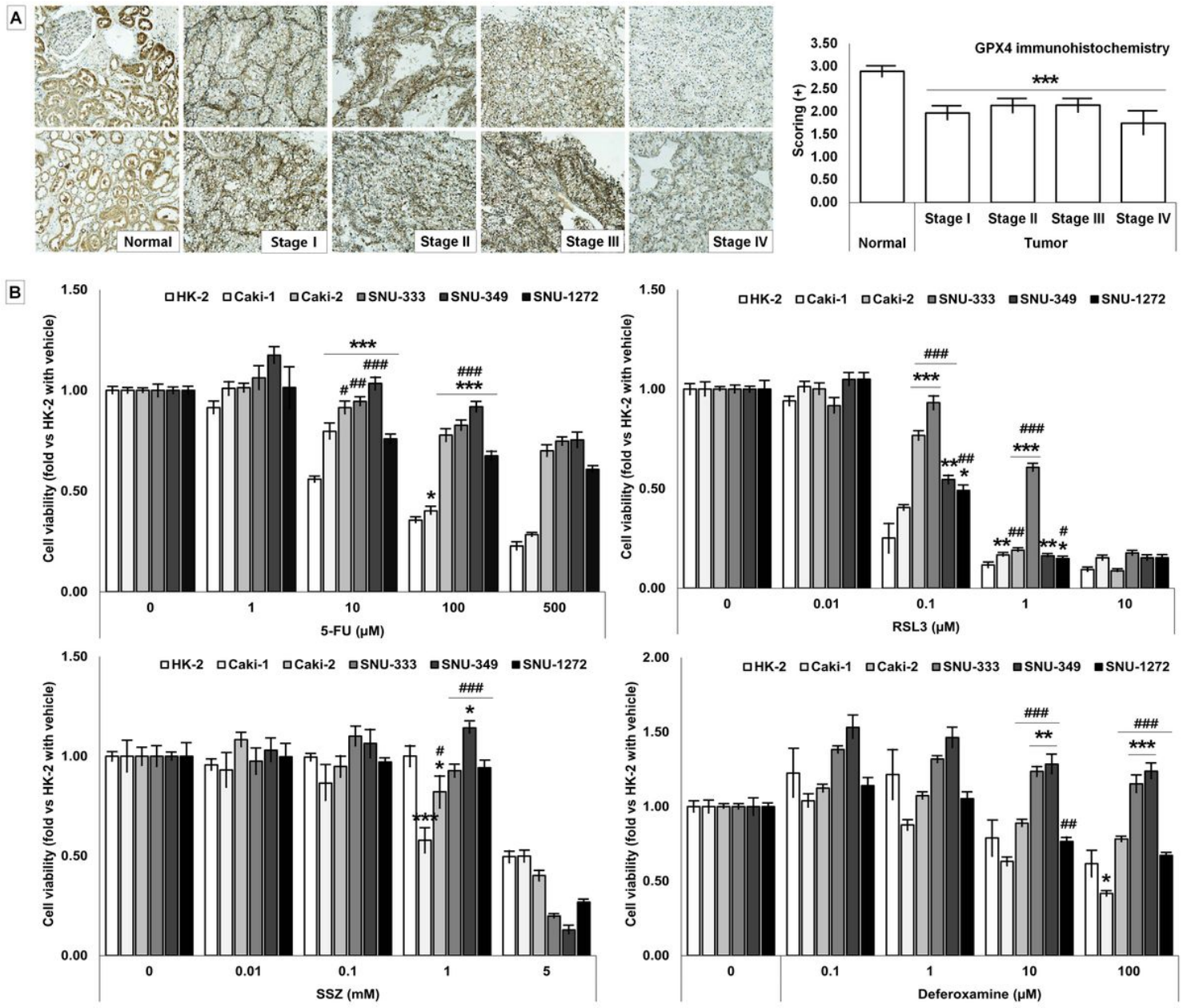

Figure 1

GPX4 immunostaining of human RCC tissue array and cell viability of RCC cells treated with related chemicals A. Expression of GPX4 in human primary RCC (Stage I, 20 cases; Stage II, 11 cases; Stage III, 14 cases), metastatic RCC tissues (Stage IV, 4 cases), and matching normal kidney tissue (nine cases). Representative photographs are shown (x 100) and staining intensity was scored and presented as mean values ± SD. ***Compared to normal adjacent kidney ($P < 0.001$) B. Effects of 5-FU, RSL3 (GPX4 inhibitor), sulfasalazine (xCT inhibitor), and deferoxamine on cell viability were assessed using an MTT assay. All RCC cell lines showed considerably higher IC50 values with 5-FU and RSL3 compared to the HK-2 cells, and primary the RCC cell lines also showed significance compared to the metastatic RCC cells, Caki-1. Metastatic RCC Caki-1 cells showed significantly lower IC50 values with sulfasalazine and deferoxamine compared to the HK-2 cells, but the primary RCC cell lines showed considerably higher IC50

values compared to the HK-2 and Caki-1 cells, respectively. *p < 0.05, **p < 0.01, and ***p < 0.001 versus HK-2 #p < 0.05, ##p < 0.01, and ###p < 0.001 versus Caki-1

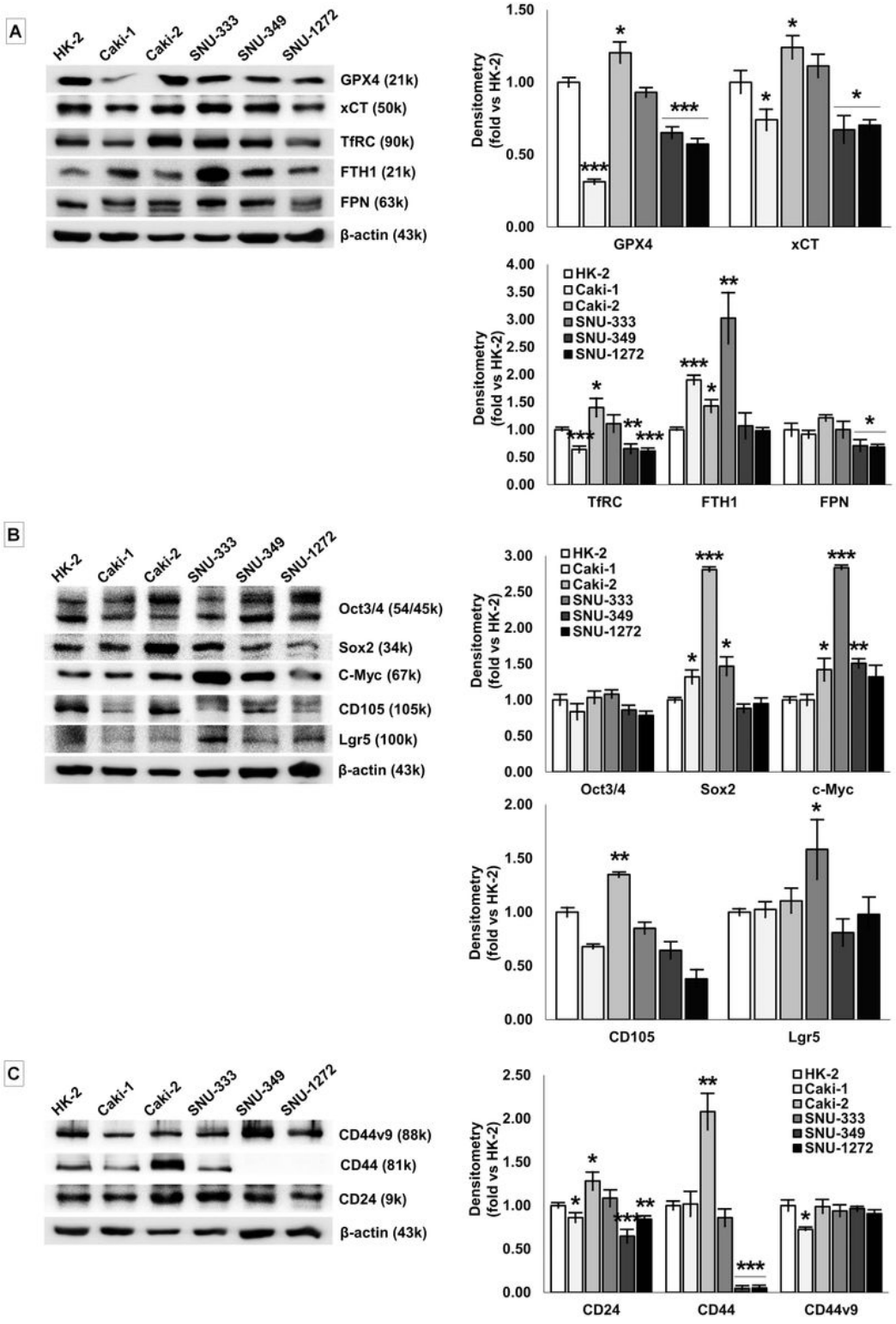

Figure 2

Quantitative results with ferroptosis, cancer stem cell markers, and tumor markers related to RCC A. Representative images of Western blots and densitometry of ferroptosis-related markers. The Caki-2 cells showed significantly increased levels of GPX4, xCT, TfRC, and FTH1, whereas the Caki-1 cells showed

decreased levels of GPX4, xCT, and TfRC compared to the HK-2 cells. The SNU-333 cells showed significantly increased levels of FTH1, while the other markers were comparable to those of the HK-2 cells. B. Representative images of Western blots and densitometry of the cancer stem cell and tumor markers. The Caki-2 cells showed significantly increased levels of Sox2, c-Myc, and CD105, while the Caki-1 cells showed decreased levels of Sox2 compared to the HK-2 cells. The SNU-333 cells showed significantly increased levels of Sox2, c-Myc, and Lgr5. C. Representative images of Western blots and densitometry of the surface markers. The Caki-2 cells showed significantly increased levels of CD24 and CD44, while others showed decreased or levels comparable to those of the HK-2 cells. *$p < 0.05$, **$p < 0.01$, ***$p < 0.001$ versus HK-2

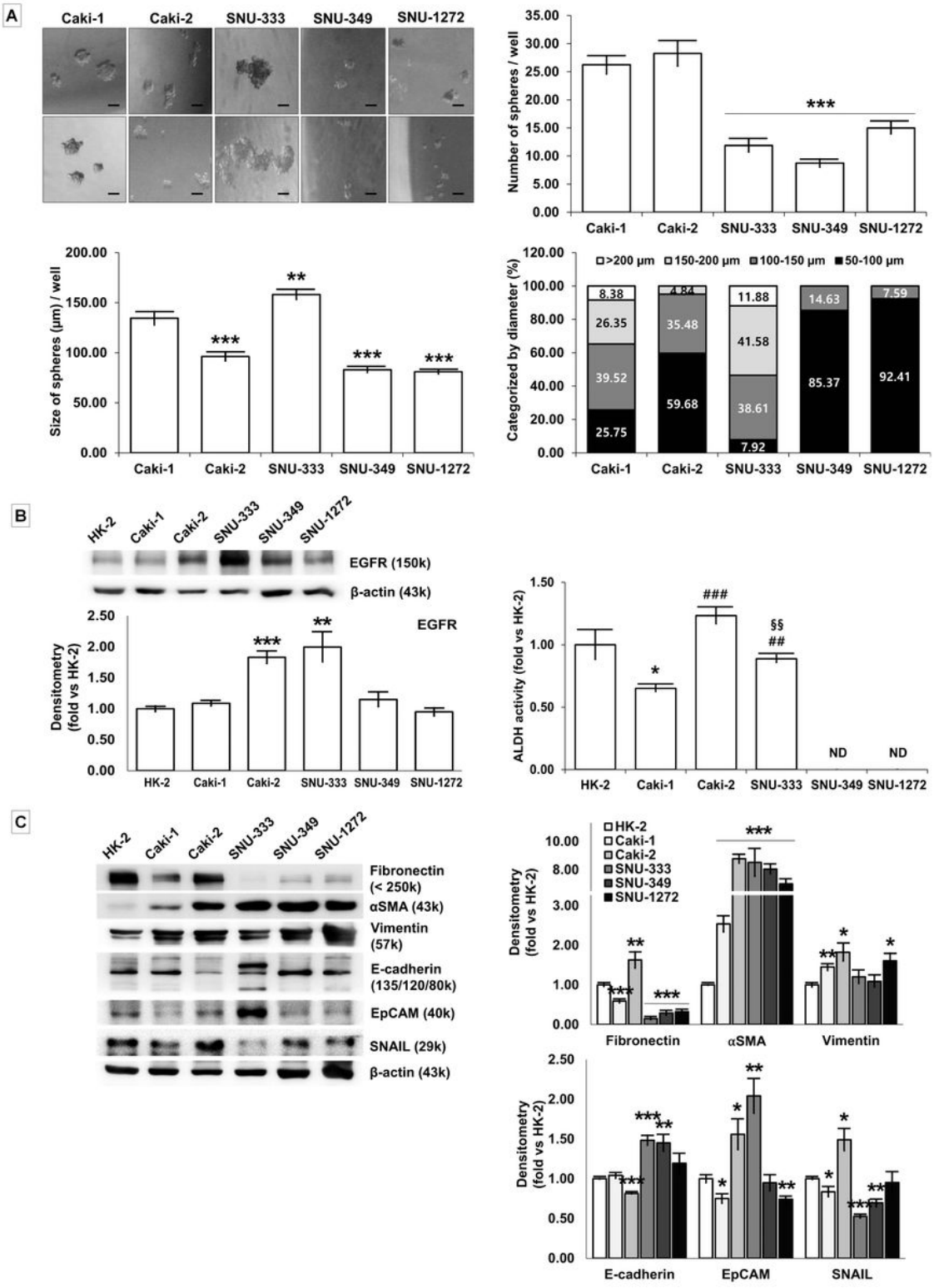

Figure 3

Sphere formation and tumorigenic capacity of RCC cell lines A. Representative images of the morphology of the renospheres growing in suspension culture in serum-free media supplemented with growth factors. The number of renospheres was significantly lower in the SNU-333, SNU-349, and SNU-1272 cells compared to the Caki-1 cells. The mean size of the renospheres was bigger in the SNU-333 cells compared to the Caki-1 cells, in which the percentage of large renospheres (> 100 μm) was the highest in

the SNU-333 cells. Scale bar = 100 μm B. Representative images of Western blots and densitometry with EGFR. The Caki-2 and SNU-333 cells showed significantly increased levels of EGFR compared to the HK-2 cells. The Caki-2 and SNU-333 cells showed considerably increased ALDH activity compared to the Caki-1cells. C. Representative images of Western blots and densitometry of the EMT markers. All RCC cell lines showed significantly higher levels of αSMA. The Caki-2 cells showed significantly increased levels of fibronectin, vimentin, and SNAIL, while the SNU-333 cells showed significantly increased levels of E-cadherin and EpCAM compared to the HK-2 cells. *p < 0.05 versus HK-2; ##p < 0.01, and ###p < 0.001 versus Caki-1; §§p < 0.01 versus Caki-2

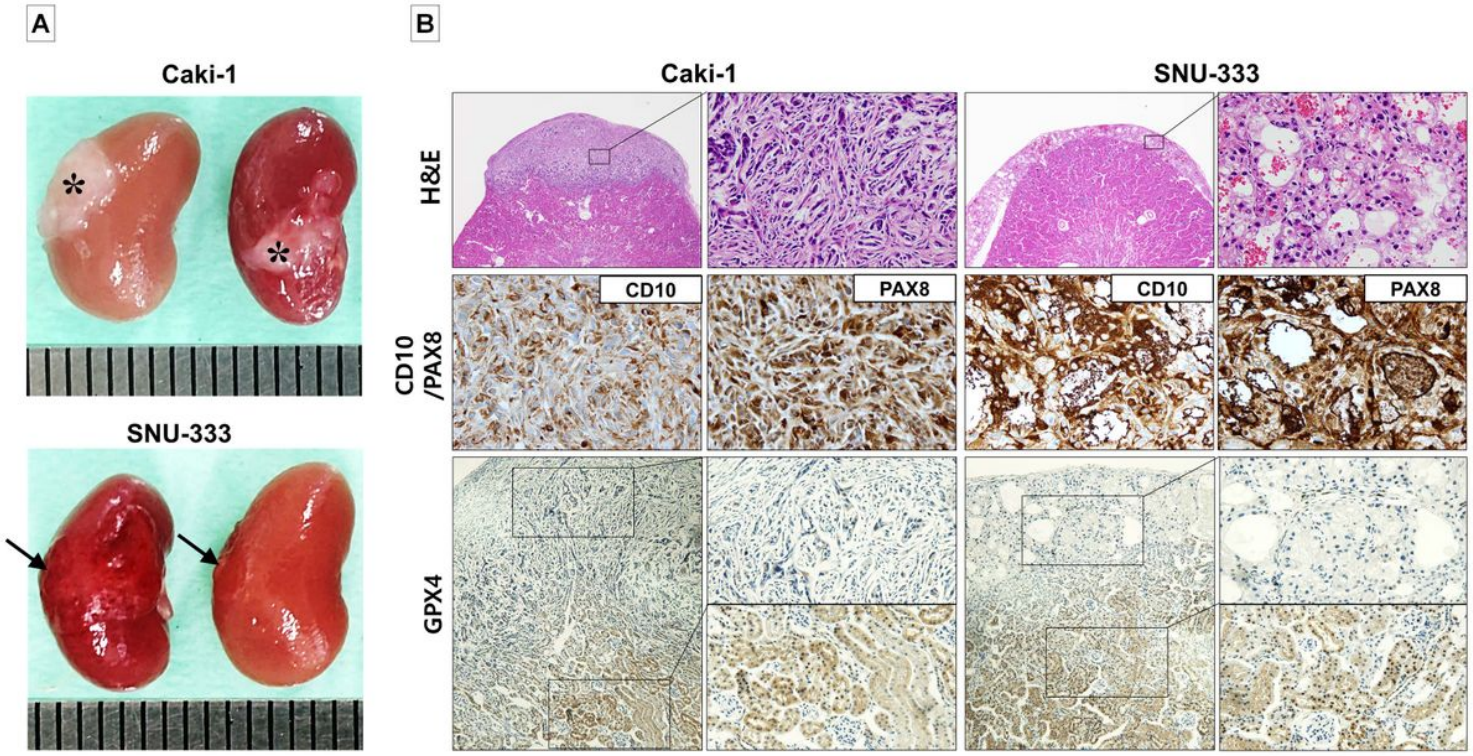

Figure 4

Orthotopic RCC model establishment from RCC cell line injection A. Representative images of the orthotopic RCC masses. The Caki-1 (asterisk) and SNU-333 (arrow) cells induced orthotopic RCC masses among the RCC cell lines in Balb/c nude mice. B. Representative images of H/E and immunohistochemistry (IHC). The Caki-1-bearing tumors consisted of spindle tumor cells with marked nuclear pleomorphism and desmoplasia and showed focal CD10 and PAX8 immunopositivity. The SNU-333-bearing tumors consisted of epithelioid tumor cells with clear or granular cytoplasm and showed strong CD10 and PAX8 immunopositivity (H/E x 40, IHC x 200). The staining intensity of GPX4 was considerably weaker in both orthotopic tumor masses (upper panel) compared to normal murine kidney (lower panel). left x100, right x200